

# Ergodicity breaking and particle spreading in noisy heterogeneous diffusion processes

Andrey G. Cherstvy<sup>1</sup> and Ralf Metzler<sup>1,2</sup>

<sup>1</sup>*Institute for Physics & Astronomy, University of Potsdam, 14476 Potsdam-Golm, Germany\**

<sup>2</sup>*Department of Physics, Tampere University of Technology, 33101 Tampere, Finland†*

(Dated: 3rd August 2021)

We study noisy heterogeneous diffusion processes with a position dependent diffusivity of the form  $D(x) \sim D_0|x|^\alpha$  in the presence of annealed and quenched disorder of the environment, corresponding to an effective variation of the exponent  $\alpha$  in time and space. In the case of annealed disorder, for which effectively  $\alpha = \alpha(t)$  we show how the long time scaling of the ensemble mean squared displacement (MSD) and the amplitude variation of individual realizations of the time averaged MSD are affected by the disorder strength. For the case of quenched disorder, the long time behavior becomes effectively Brownian after a number of jumps between the domains of a stratified medium. In the latter situation the averages are taken over both an ensemble of particles and different realizations of the disorder. As physical observables we analyze in detail the ensemble and time averaged MSDs, the ergodicity breaking parameter, and higher order moments of the time averages.

PACS numbers: 05.40.-a

## I. INTRODUCTION

The motion of individual molecules and submicron tracer particles of different sizes in the cytoplasm of living biological cells [1], in artificially crowded environments in vitro [2], in glass-like systems [3], or in large scale in silico studies of membrane structures [4] was shown to follow the anomalous diffusion law

$$\langle x^2(t) \rangle \simeq t^\beta, \quad (1)$$

with the subdiffusive diffusion exponent mostly in the range  $\beta = 0.4 \dots 0.9$  [5, 6]. A number of mathematical models of different kinds were proposed to unveil the properties of anomalous diffusion phenomena embodied in the mean squared displacement (MSD) in Eq. (1) [7]. In most of these models the properties of the stochastic process are homogeneous in space. Especially for smaller tracers, which may cover longer distances within the measurement time, or for techniques allowing for full maps of local diffusivities, it turns out that the diffusion coefficient becomes a function of the local tracer position. For both eukaryotic [8] and prokaryotic [9] cells such local diffusivity maps indeed show significant variations. The motion of tracer particles through space may also be impeded by caging effects when the size of the particle is comparable to the local mesh size in structured environments [10, 11]. In such cases the tracer diffusion becomes characterized by a non-uniform, position-dependent diffusivity  $D(x)$ . Similarly, spatially varying transport characteristics are ubiquitous in contaminant dispersion in subsurface water aquifers [12].

In the field of stochastic dynamics anomalous diffusion in spatially random media, disordered energy landscapes,

weakly chaotic systems, and dynamic maps received considerable attention [13–20]. More specifically, anomalous diffusion due to micro-domains was investigated [21] and the influence of environmental Gaussian noise on diffusive particle trajectories in disordered systems was studied [22]. Moreover, deviations from normal diffusion due to quenched and annealed disorder of the medium diffusivity received renewed interest [23, 24]. In such studies one is mainly interested in the quantitative behavior of the particle MSD (1) as well as the ergodic properties of the system: is the information from time averages of physical observables typically garnered as time series by modern particle tracking assays equivalent to those of the corresponding ensemble averages known from the theoretical models? It turns out that a large variety of anomalous diffusion processes involve weak ergodicity breaking [7, 25–29], the disparity between (long) time averages and ensemble averages of physical observables such as the MSD, and that in those cases the Khintchine theorem needs to be substituted by generalized versions [30, 31].

Here, we study the dynamics and the ergodic properties of heterogeneous diffusion processes (HDPs) with position dependent diffusivity  $D(x)$ , in the presence of piece-wise deterministic quenched and annealed disorder. More specifically, we generalize HDPs with power-law diffusivity

$$D(x) = D_0|x|^{\alpha_0}, \quad (2)$$

for which the anomalous diffusion exponent of the MSD assumes the form [32–36]

$$\beta = \frac{2}{2 - \alpha_0}. \quad (3)$$

The physical dimension of the coefficient  $D_0$  in Eq. (2) is  $[D_0] = \text{cm}^{2-\alpha_0}\text{sec}^{-1}$ . The exponent (3) designates subdiffusion for  $\alpha_0 < 0$  and superdiffusion for  $0 < \alpha_0$  [32–36]. The profiles of the diffusivity for these cases are shown in Fig. 1a,b. HDPs are weakly non-ergodic and ageing,

\*Electronic address: a.cherstvy@gmail.com

†Electronic address: rmetzler@uni-potsdam.de

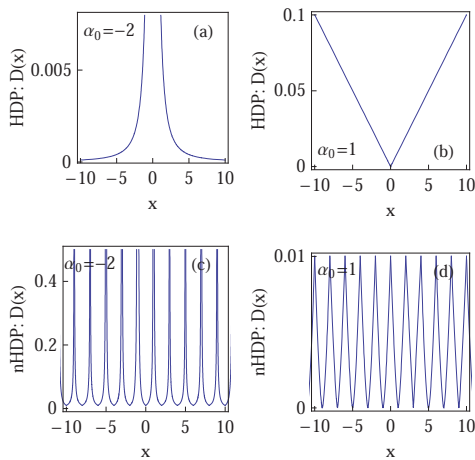


Figure 1: Particle diffusivity for heterogeneous diffusion processes: (a) and (b) for, respectively,  $\alpha_0 = -2$  and  $\alpha_0 = 1$ . Panels (c) and (d) show the diffusivity of HDPs with quenched disorder for the same values of  $\alpha_0$  and for the parameters  $\sigma^2 = 0.25$  and  $2\delta x = 2$  (see text for details). Slight variations of the diffusivity in panels (c) and (d) indicate the external noise superimposed in the process.

that is, their dynamics depends explicitly on the time gap between original initiation of the system and start of the measurement [32–36]. We note that the ageing properties of HDPs [35] embodied in the ensemble and time averaged MSDs are in fact similar to those of subdiffusive continuous time random walks [37] and scaled Brownian motion [38].

In the following we unravel how the additional disorder in the system modifies the diffusive and ergodic properties of HDPs. We compute the scaling laws for the ensemble and time averaged MSDs as well as the amplitude spread of individual realizations of the process. The article is structured as follows. In Sec. II we define the observables, that we will analyze. Sec. III specifies the model and its implementation in the simulations. In Sec. IV we then study HDPs with annealed disorder, followed by the scenario with quenched disorder in Sec. V. Sec. VI concludes this work.

## II. OBSERVABLES

The central quantity in the study of stochastic processes is the ensemble averaged MSD

$$\langle x^2(t) \rangle = \int_{-\infty}^{\infty} x^2 P(x, t) dx, \quad (4)$$

calculated as the spatial average of  $x^2$  over the probability density function  $P(x, t)$  to find the particle at position  $x$  at given time  $t$  [39]. However, when individual time series  $x(t)$  of the particle position are measured in experiments or simulations, the typical quantity studied

is the time averaged MSD

$$\overline{\delta^2(\Delta)} = \frac{1}{T - \Delta} \int_0^{T - \Delta} [x(t + \Delta) - x(t)]^2 dt. \quad (5)$$

Here  $\Delta$  is the lag time and  $T$  is the measurement time (length) of the trajectory  $x(t)$  [7, 27, 28]. Often, also the additional average

$$\langle \overline{\delta^2(\Delta)} \rangle = \frac{1}{N} \sum_{i=1}^N \overline{\delta_i^2(\Delta)} \quad (6)$$

of the time averaged MSD over  $N$  individual trajectories is taken [7, 27, 28]. A process is called ergodic when we observe the equality

$$\langle x^2(\Delta) \rangle = \lim_{\Delta/T \rightarrow 0} \overline{\delta^2(\Delta)}. \quad (7)$$

Examples for ergodic processes are Brownian motion [7, 27–29] as well as anomalous diffusion processes with MSD (1) given by random walks on fractals [40] and processes driven by fractional Gaussian noise [41–43]. Once a process is non-stationary, the equality (7) is violated, the phenomenon of weak ergodicity breaking [7, 25–29]. A whole range of anomalous diffusion processes with power-law MSD (1) belongs to this class and specifically exhibits the linear lag time dependence

$$\langle \overline{\delta^2(\Delta)} \rangle \simeq \frac{\Delta}{T^{1-\beta}} \quad (8)$$

of the time averaged MSD [7]. As examples we mention continuous time random walk processes with scale free distributions of waiting times [7, 25–29, 31], correlated continuous time random walks [44], as well as diffusion processes with space [32–36] and time [32, 38, 45, 46] dependent diffusion coefficients and their combinations [47]. We also mention ultraslow diffusion processes with a logarithmic form for  $\langle x^2(t) \rangle$  and linear lag time dependence (8) of the time averaged MSD [48] as well as the ultraweak ergodicity breaking of superdiffusive Lévy walks [49].

For finite measurement time even ergodic processes exhibit a statistical scatter of the amplitude of time averaged observables. This irreproducibility for the case of the time averaged MSD  $\overline{\delta^2(\Delta)}$  can be quantified in terms of the distribution  $\phi(\xi)$  as function of the dimensionless variable [7, 26–28]

$$\xi = \frac{\overline{\delta^2}}{\langle \overline{\delta^2} \rangle}. \quad (9)$$

The variance of  $\phi(\xi)$  is quantified in terms of the ergodicity breaking parameter [7, 26–28]

$$\text{EB}(\Delta) = \langle \xi^2(\Delta) \rangle - \langle \xi(\Delta) \rangle^2 \equiv \langle \xi^2 \rangle - 1. \quad (10)$$

For Brownian motion the behavior of the ergodicity breaking parameter at  $\Delta/T \rightarrow 0$  is

$$\text{EB}_{\text{BM}}(\Delta) = \frac{4\Delta}{3T}. \quad (11)$$

Continuous time random walk processes with scale free waiting time distribution have a finite value for EB even in the limit  $\Delta/T = 0$  [26], similar to HDPs [33–36], while for scaled Brownian motion the ergodicity breaking parameter approaches zero in this limit [45, 46].

For reference in what follows we also mention that the probability density function of HDPs obeys has the exponential form [33]

$$P(x, t) = \frac{|x|^{-2/\alpha_0}}{\sqrt{4\pi D_0 t}} \exp\left(-\frac{|x|^{2-\alpha_0}}{(2-\alpha_0)^2 D_0 t}\right) \quad (12)$$

which is a stretched (compressed) Gaussian for superdiffusive (subdiffusive) HDPs with  $0 < \alpha_0 < 2$  ( $\alpha_0 < 0$ ). Note that, respectively, the shape (12) has a distinct cusp at the origin or is bimodal with  $P(0, t) = 0$  [33].

### III. MODEL

We employ the same tested stochastic algorithm for the Markovian HDPs as developed in Refs. [33–36], based on the one-dimensional Langevin equation for the particle displacement  $x(t)$  with the position dependent diffusivity  $D(x)$ ,

$$\frac{dx(t)}{dt} = \sqrt{2D(x)} \times \zeta(t). \quad (13)$$

The process is driven by the white Gaussian noise  $\zeta(t)$  with covariance  $\langle \zeta(t)\zeta(t') \rangle = \delta(t-t')$  and zero mean  $\langle \zeta(t) \rangle = 0$ . We interpret Eq. (13) in the Stratonovich sense leading to the following implicit mid-point iterative scheme: at step  $i+1$  the particle position is

$$x_{i+1} - x_i = \sqrt{2D\left(\frac{x_{i+1} + x_i}{2}\right)} \times (y_{i+1} - y_i), \quad (14)$$

where the increments  $(y_{i+1} - y_i)$  of the Wiener process represent a  $\delta$ -correlated Gaussian noise with unit variance and zero mean. Unit time intervals separate consecutive iteration steps. Below we simulate three values for the exponent  $\alpha_0$ , corresponding to  $\beta = 1/2$  (subdiffusive MSD),  $\beta = 0$  (Brownian motion), and  $\beta = 2$  (superdiffusive MSD). For standard HDPs these cases were analyzed by us in Refs. [33–36]. To avoid divergencies of the particle motion we regularize the diffusivity at  $x = 0$  by addition of a small constant, namely  $D(x) = D_0(|x|^\alpha + D_{\text{off}})$  where  $D_{\text{off}} = 10^{-3}$  and  $D_0 = 10^{-2}$  for all results shown below. This choice does not affect the quality of the studied scaling laws [33].

To examine the effect of additional noise due to the environment we implement a Gaussian distribution of the scaling exponent of the diffusivity with the mean  $\alpha_0$ ,

$$p(\alpha) = \frac{1}{\sqrt{2\pi\sigma^2}} \exp\left(-\frac{(\alpha - \alpha_0)^2}{2\sigma^2}\right). \quad (15)$$

Generally, the distribution  $p(\alpha)$  may be asymmetric, but we restrict our discussion to symmetric forms. We consider two versions of this additional disorder corresponding to the annealed and quenched limits for the variation of  $\alpha$ . In the annealed case of noisy HDPs, the properties of the environment change rapidly in time compared to time scales of the particle motion. Physically, such noise may be due to the imprecision of the experimental setup or because of additional thermal agitation in the system. The diffusing particle thus visits regions in space with different local exponents  $\alpha$ . In this scheme the particle diffusivity at position  $x$  fluctuates in time, and the value of the diffusivity will be different each time the particle revisits the same position  $x$ . In this annealed case large diffusivity variations occur in the entire space.

In superdiffusive HDPs distant particle excursions take place due to the growth of  $D(x)$  away from the origin and the associated acceleration of the motion, while for subdiffusive HDPs the walker is increasingly trapped in the low-diffusivity regions at larger value of the position  $|x|$  [33–36]. With increasing strength  $\sigma^2$  of the annealed noise given by the distribution (15) the excursions of the particles in both superdiffusive and subdiffusive cases become more erratic as time evolves. The time interval  $\delta t$  during which the walker has a given HDP exponent  $\alpha_i$  obviously affects the properties of noisy HDPs. These time spans  $\delta t$  are here taken to be uniformly distributed. To simulate annealed noisy HDPs we use Eq. (15) with varying  $\sigma^2$ . The particle performs jumps with a given scaling exponent for the time interval  $\delta t$ , after which a new exponent is chosen from the distribution (15), and so on. The particle displacement  $x_i$  during the time span  $(t_i, t_i + \delta t)$  with HDP exponent  $\alpha_i$  is the starting condition for the next time interval. Shorter  $\delta t$  intervals imply more erratic motion, as shown below.

For noisy HDPs in the presence of quenched disorder, the profile of the particle diffusivity is hard-wired into the environment. We choose a static periodic arrangement of domains as shown in Fig. 1c,d. In each domain the exponent  $\alpha$  is drawn from  $p(\alpha)$  and the particle performs a regular HDP. The midpoint of each domain is chosen as the origin in the local HDP coordinate system, that is, locally the functional shape of  $D(x)$  is centered and decays or increases with the local scaling exponent  $\alpha$ , as exemplified in Fig. 1c,d. The period  $\delta x$  for the stratification of the environment plays the role of a switching mechanism affecting the system dynamics. At the boundary of the domains the diffusivity and its derivative in general acquire jumps. Physically, the latter occurs in the presence of some walls, cages, etc.

We simulate quenched noisy HDPs as follows. The entire space is stratified into domains of width  $2\delta x$ , and the local HDP exponent is chosen from the distribution (15). The length  $\delta x$  is a vital parameter of quenched noisy HDPs. The particle performs an HDP random walk in each space domain with  $D(x, \alpha)$  and it hops to a neighboring domain once the domain boundary is reached. The centers of the domains are computed from

the particle position  $x_i$  as

$$x_{c,i} = 2(\delta x) \text{int} \left[ \frac{x_i}{2\delta x} \right] + \text{sign}[x_i](\delta x), \quad (16)$$

see Fig. 1c,d. Here  $\text{int}[x]$  denotes the integer part of the argument, and an additional  $\delta x$  shift is used for convenience. The starting position of the particle is near the center of the first domain, at  $x(0) = 0.1 + x_{c,1}$ . The subsequent position  $x_{i+1}$  is evaluated from  $x_i$  with the local exponent  $\alpha_i$  according to Eq. (14), that is,

$$x_{i+1} - x_i = \sqrt{2D_0 \left( \left| \frac{x_{i+1} + x_i}{2} - x_{c,i} \right|^{\alpha_i} + D_{\text{off}} \right)} \times (y_{i+1} - y_i). \quad (17)$$

We vary the width of  $p(\alpha)$  and the mean value of the scaling exponent  $\alpha_0$ . Shorter periodicities  $\delta x$  are equivalent to stronger external noise, as shown below. We note here that for subdiffusive HDPs the centers of the domains  $x_{c,i}$  correspond to the regions of maximal diffusivity, while for superdiffusive HDPs these are the spots of the lowest diffusivity [33, 34].

#### IV. NOISY HDPS WITH ANNEALED DISORDER

##### A. Noisy Brownian motion, $\alpha_0 = 0$

For  $\alpha_0 = 0$  and a small value  $\sigma^2$  of the additional noise, as expected, we observe small discrepancies from the canonical Brownian motion, as evidenced in Fig. 2b. The behavior is ergodic, and the ergodicity breaking parameter follows the known behavior (11) for Brownian motion, see Fig. 3. Most importantly, the ensemble averaged MSD equals the time averaged MSD, apart from very short lag times at which the relaxation from the initial value  $x(0) = x_0$  occurs (compare Ref. [35] for more details). At longer lag times, the deteriorating statistics of the  $\overline{\delta^2}$  traces give rise to the typical cone-like scatter.

As the noise strength  $\sigma^2$ , the variance of the  $\alpha$  distribution  $p(\alpha)$  is increased, see, for instance, in the panel for the noise strength  $\sigma = 0.5$  in Fig. 2b: a more pronounced scatter of the  $\overline{\delta^2}$  traces emerges and, importantly, persists in the limit  $\Delta/T \rightarrow 0$ . The occurrence of progressively more distant particle excursions caused by superdiffusive traces with  $\alpha > 0$  gives rise to a larger spread of the amplitude scatter quantified by the distribution  $\phi(\xi)$ . The value of  $\langle \overline{\delta^2} \rangle$  grows somewhat faster than the ensemble MSD (1) due to these outliers, giving rise to larger values of the ergodicity breaking parameter EB (not shown). The time averaged MSD  $\overline{\delta^2}(\Delta)$  scales linearly with the lag time  $\Delta$ , and, as they should, in the limit  $\Delta \rightarrow T$  the time averaged MSD settles back to the ensemble averaged MSD, due to the pole in the definition (5) of the time average.

For even larger noise strength  $\sigma^2$ , the behavior of the time averaged MSD and the ergodic properties are dominated by extreme events, that is, by single or few trajectories in the data set with the largest exponent(s) yielding extremely distant particle excursions. With an increasing width of the  $\alpha$  distribution  $p(\alpha)$ , the spread of the time averaged MSD grows, as well, as evidenced in Fig. 2b. Similarly, for such large values of the noise strength  $\sigma^2$  the value of the ergodicity breaking parameter becomes proportional to the number  $N$  of recorded traces, witnessing the dominance of single traces, each having the potential to be more extreme than the others, compare Fig. 3a. We refer the reader to Ref. [35], in which the critical properties of HDPs and the effects of the number of traces are analyzed in the limit  $\alpha_0 \rightarrow 2$ .

For narrow distributions  $p(\alpha)$  the spread  $\phi(\xi)$  of individual  $\overline{\delta^2}$  traces is symmetric at short lag times  $\Delta$ , developing a tail at larger lag times  $\Delta$ . This behavior can be rationalized in terms of a generalized Gamma distribution (see Ref. [33]). The general features of  $\phi(\xi)$  are shown in Fig. 3 in terms of the higher moments of this distribution. These are the skewness

$$S(\xi) = \frac{N^{-1} \sum_{i=1}^N (\xi - 1)^3}{\left( N^{-1} \sum_{i=1}^N (\xi - 1)^2 \right)^{3/2}} \quad (18)$$

and the kurtosis

$$K(\xi) = \frac{N^{-1} \sum_{i=1}^N (\xi - 1)^4}{\left( N^{-1} \sum_{i=1}^N (\xi - 1)^2 \right)^2}, \quad (19)$$

which complement the variance of  $\phi(\xi)$  described by the ergodicity breaking parameter (10). In Fig. 3a we also observe that for small noise strengths  $\sigma^2$  the value  $\text{EB}(\Delta = 1)$  for noisy Brownian motion approaches  $\text{EB}_{\text{BM}}(\Delta = 1)$  given by Eq. (11), as expected. The values of the ergodicity breaking parameter grow with  $\Delta$ , indicative of a bigger spread of the value  $\overline{\delta^2}$  of individual traces (green points in Fig. 3a).

##### B. Subdiffusive noisy HDP, $\alpha_0 = -2$

For the subdiffusive case the time evolution of the ensemble and time averaged MSDs is illustrated in Fig. 2a for different noise strengths  $\sigma^2$  of the  $\alpha$  distribution. We observe that for the subdiffusive value  $\alpha_0 = -2$  the same magnitude of the  $\alpha$  variation causes a much weaker effect as compared to the Brownian ( $\alpha_0 = 0$ ) or superdiffusive ( $\alpha_0 = 1$ ) situations. The scatter of  $\overline{\delta^2}$  remains nearly insensitive to the lag time  $\Delta$ , similar to canonical HDPs [33, 35]. The scaling of the ensemble averaged MSD also agrees with that for HDPs [33]. It is reached after less than a dozen of steps during which the relaxation of the initial condition occurs, compare Refs. [33, 35]. The scaling of the time averaged MSD  $\langle \overline{\delta^2} \rangle$  remains linear and

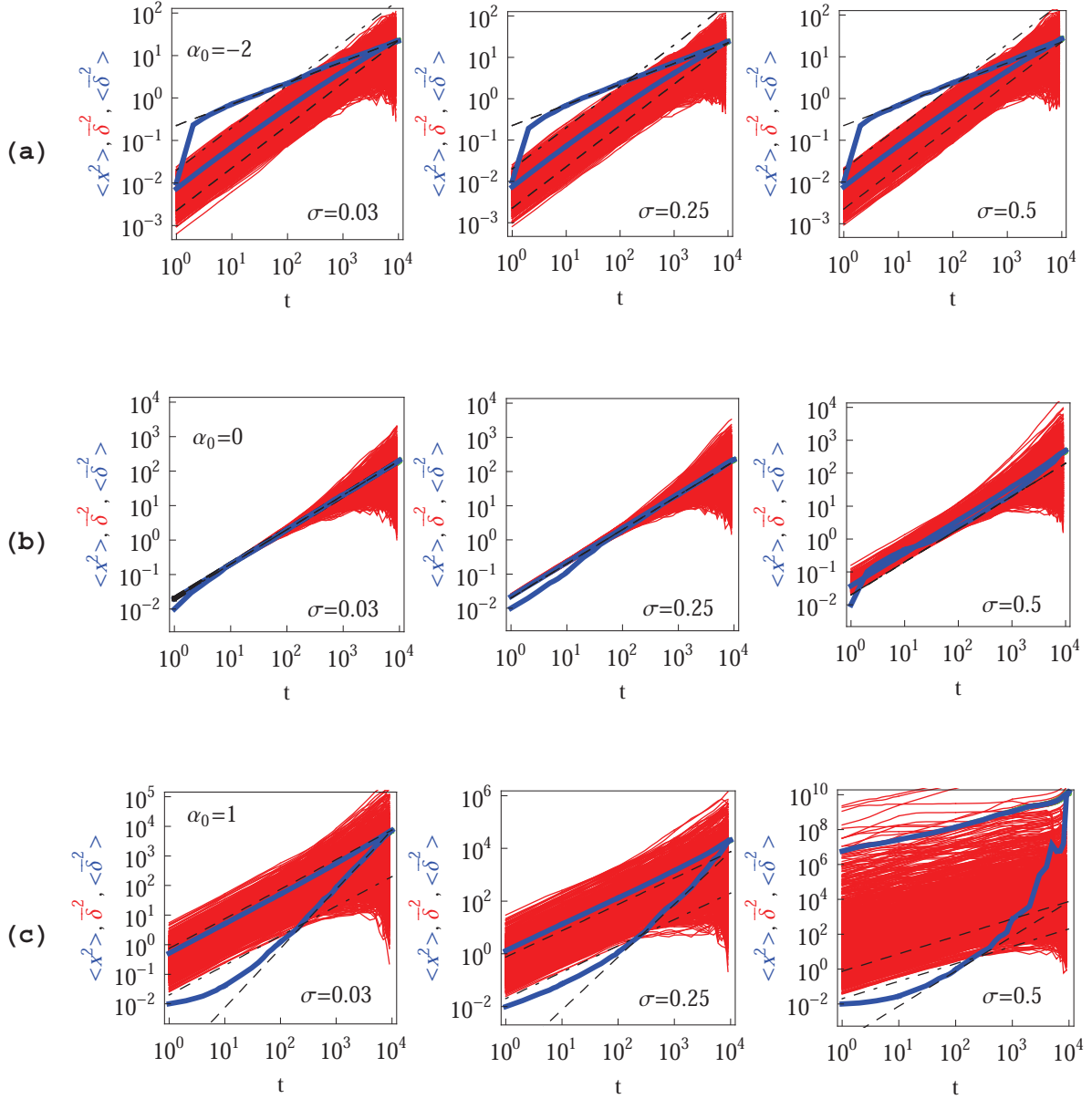


Figure 2: Ensemble and time averaged MSDs  $\langle x^2(t) \rangle$  and  $\langle \overline{\delta^2(\Delta)} \rangle$  (thick blue curves) as well as individual time averaged MSDs  $\overline{\delta^2}$  (red curves) for annealed noisy HDPs. Parameters: the values of  $\alpha_0$  and its variance are indicated in the plots, the trace length is  $T = 10^4$ , and the number of sampled traces is  $N = 10^3$ . The initial position is  $x_0 = x(t=0) = 0.1$ . The top panels correspond to the noisy subdiffusive case, the middle panel represents noisy Brownian motion, and the bottom panels are the case of superdiffusive noisy HDPs. The asymptotes (1) and (8) for the ensemble and time averaged MSDs of standard HDPs are shown as the dashed curves. The Brownian asymptote  $\langle x^2(t) \rangle = 2D_0 t$  is the dashed-dotted line.

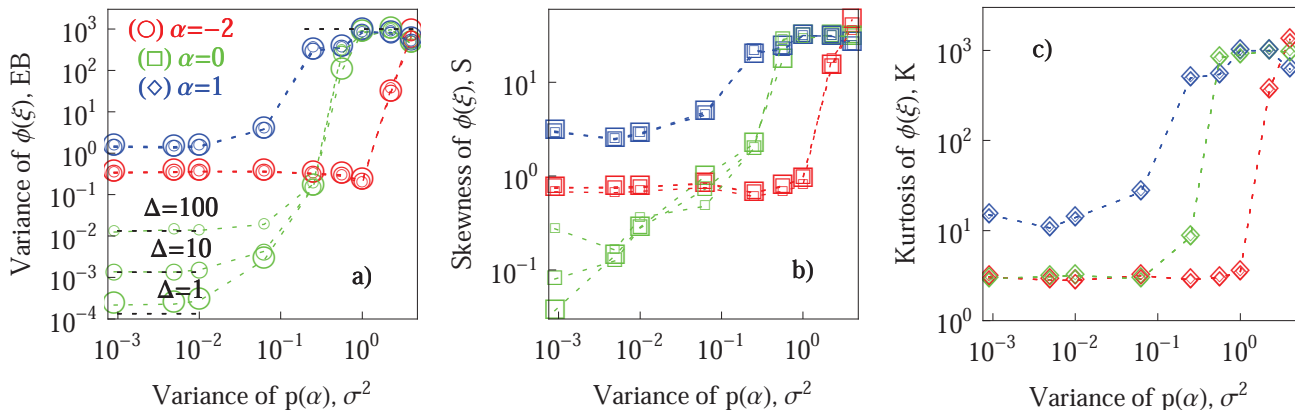


Figure 3: Second, third, and fourth order moments of the amplitude scatter distribution  $\phi(\xi)$  for annealed noisy HDPs, computed for the parameters of Fig. 2. Large, medium, and small symbols correspond to lag times  $\Delta = 1, 10,$  and  $100$ , respectively. The dotted line in panel (a) at large  $\sigma^2$  is the ergodicity breaking parameter  $EB \approx N = 10^3$ , indicative of the single trace dominance in this case, see text. The dotted lines in panel (a) for small noise strength  $\sigma^2$  stands for  $EB_{BM}(\Delta)$  given by Eq. (11).

nearly unaffected by changes of  $\sigma^2$ . The long time scaling of the MSD is also weakly sensitive to  $\sigma^2$  in the range considered here.

Physically, for the subdiffusive case the spread of  $\alpha_i$  should be  $\gtrsim \alpha_0$  to give rise to fast particle excursions (outliers). Thus, much larger  $\sigma^2$  values are required to disturb the spread of  $\bar{\delta}^2$  for strongly subdiffusive noisy HDPs as compared to superdiffusive noisy HDPs shown in Fig. 2c. This is our first important conclusion.

We rationalize the effects of the  $\alpha$  spread further in terms of the width and higher moments of the amplitude scatter distribution  $\phi(\xi)$ . The results for  $\alpha_0 = 0$ , sub- and superdiffusive annealed noisy HDPs are shown in Fig. 3a. We observe that all moments are typically smaller for the subdiffusive case reflecting a less pronounced and asymmetric spread of  $\bar{\delta}^2$ . The skewness of Brownian

motion ( $\sigma^2 \rightarrow 0$ ) tends to vanish, as it should, while for sub- and superdiffusive noisy HDPs it attains finite values at  $\sigma^2 \rightarrow 0$  (Fig. 3b). This is due to the inherent asymmetry of the  $\phi(\xi)$  scatter even at  $\sigma^2 \rightarrow 0$ : it features a tail at large  $\xi$  values, a maximum at intermediate  $\xi$ , and vanishes at  $\xi \rightarrow 0$  [33]. Both skewness  $S(\xi)$  and kurtosis  $K(\xi)$  grow dramatically with  $\sigma^2$  for all values of  $\alpha_0$ , as demonstrated in Figs. 3b,c. We checked that for  $\sigma^2 \rightarrow 0$  the value of the ergodicity breaking parameter in the limit  $\Delta/T \ll 1$  approaches that for standard HDPs [33], as expected, while for a broad distribution of  $\alpha$  values the ergodicity breaking parameter increases and eventually approaches the number of traces  $N$  in the data set (single-trace domination), Fig. 3a. The value of the ergodicity breaking parameter  $EB$  for  $\alpha_0 < 0$  is nearly unaffected by variations of  $\sigma^2$  over a wide range, see the

red symbols in Fig. 3a. This reflects the minor change in the spread of single traces  $\overline{\delta^2}$  when  $\sigma^2$  is varied, see Fig. 2a.

### C. Superdiffusive noisy HDPs, $\alpha_0 = 1$

The ensemble and time averaged MSDs of superdiffusive noisy HDPs with  $\alpha_0 = 1$  are shown in Fig. 2c. For small noise strengths  $\sigma^2$  their scaling agrees with the results for standard HDPs, Eqs. (1) and (8). With increasing noise strength  $\sigma^2$ , the time averaged MSD traces  $\overline{\delta^2}$  grow dramatically, and for moderate and large lag times  $\Delta$  the time averaged MSD deviates progressively from the HDP scaling, that is ballistic for  $\alpha_0 = 1$  (Fig. 2c). The scatter of the individual time averaged MSDs  $\overline{\delta^2}$  becomes progressively larger and asymmetric as the width of  $p(\alpha)$  increases. The amplitude of the time averaged MSD traces  $\overline{\delta^2}$  for large values of  $\sigma^2$  grows significantly above the asymptote for undisturbed HDPs due to single trajectory domination. Therefore, the moments of the scatter distribution  $\phi(\xi)$  increase, see the blue symbols in Fig. 3. For the later parts of the trajectories, the ensemble averaged MSD increases very fast (see the right panel in Fig. 2c) to meet the value of  $\overline{\delta^2}$  in the limit  $\Delta = T$ . For superdiffusive HDPs the moments of  $\phi(\xi)$  are larger than those for subdiffusive noisy HDPs with the same  $\sigma^2$ , compare the red and blue symbols in Fig. 3.

## V. NOISY HDPs WITH QUENCHED DISORDER

We now turn to the situation of quenched disorder in a stratified environment, in which evenly sized domains of width  $\delta x$  have a diffusivity of the form (2), centered within the domain, whose  $\alpha$  value is noisy and with distribution (15). In this quenched scenario, the particle experiences the *same* value of  $\alpha$  each time it revisits a given domain. The situation is illustrated in Fig. 1c,d.

### A. Noisy Brownian motion, $\alpha_0 = 0$

For quenched, noisy Brownian motion we observe that for small noise strength  $\sigma^2$  the behavior, as expected, is very close to standard Brownian motion (not shown). For a large value of  $\sigma^2$ , the spread of the amplitude of individual time averaged MSDs  $\overline{\delta^2(\Delta)}$  is non-negligible even at short lag times  $\Delta$ , as shown in Fig. 4c. This spread is more pronounced for larger periodicities  $\delta x$  of the stratified medium. For small  $\sigma^2$  the ensemble averaged MSD  $\langle (x - x_{c,1})^2 \rangle$  computed with respect to the center of the starting domain and the time averaged MSD (thick blue lines) almost coincide for all lag times  $\Delta$  (not shown). Concurrently, the ergodicity breaking parameter follows the Brownian asymptote (11), as shown by the

green symbols in Fig. 5a. For larger values of the noise strength  $\sigma^2$  the ergodicity breaking parameter deviates pronouncedly from Eq. (11) at short lag times  $\Delta$ , indicating the occurrence of weak ergodicity breaking, along with the disparity  $\langle \overline{\delta^2} \rangle \neq \langle x^2 \rangle$ , as witnessed by Fig. 5b. This inequality is particularly pronounced for larger values of the noise strength  $\sigma^2$  and large periodicity  $\delta x$ , see the changes for varying  $\delta x$  in Fig. 4c. For wider  $\alpha$  distributions  $p(\alpha)$  the ensemble averaged MSD starts close to that of the asymptote for standard Brownian motion, while at later times there occurs a crossover to the curve for the time averaged MSD (left panel, Fig. 4c.) This behavior is also typical for sub- and superdiffusive quenched noisy HDPs, see below. For  $\sigma^2 = 1$  this transition occurs after  $\sim 10^3$  time steps and becomes less pronounced for smaller periodicities  $\delta x$  of the medium (Fig. 4c).

### B. Superdiffusive noisy HDPs, $\alpha_0 = 1$

In standard superdiffusive HDPs there exists a finite probability of particle trapping in regions of low diffusivity near the origin, as witnessed by the cusp around  $x = 0$  of the probability density function (12) [33]. For noisy HDPs we find that for large values of the domain size  $\delta x$  and small noise strengths  $\sigma^2$  the particle preferentially stays in the domain, in which it was seeded, and the resulting ensemble averaged MSD is close to that of the standard HDPs [33, 35]. Here we again computed the MSD with respect to the center  $x_{c,1}$  of the seed domain in the form  $x(t=0) - x_{c,1} = 0.1$ . The time averaged MSD is equally close to the asymptote (8) of the normal HDP. Ensemble and time averaged MSDs converge at long lag times  $\Delta \rightarrow T$ , note that the ensemble averaged MSD here is below the time averaged MSD, as evidenced by Figs. 4a,b.

We start with a narrow spread of  $\alpha$  in the spatial domains corresponding to  $\sigma = 0.03$ . In this case we find that with decreasing domain size  $\delta x$  the amplitude scatter of individual time averaged MSDs shrinks and the amplitude of the trajectory mean  $\langle \overline{\delta^2(\Delta)} \rangle$  drops substantially (Fig. 4a). The reason is that for a small domain size there are almost no regions of fast diffusivity. For small values of  $\delta x$  the ensemble and time averaged MSDs converge and drop below the Brownian asymptote, see the dashed-dotted line in the right graph in Fig. 4a. In such cases of smaller domain size the ergodicity breaking parameter attains relatively small values, as shown in Fig. 5a, indicating a more ergodic behavior. This effect of the noise is similar to that for noisy CTRWs [22]. As  $\delta x$  increases, the ergodicity breaking parameter approaches values close to those of the standard HDP,  $EB(\Delta = 1) \approx 0.34$  for  $\alpha_0 = -2$  and  $EB(\Delta = 1) \approx 1.1$  for  $\alpha_0 = 1$ , with  $T = 10^4$  [33, 35]. This is indicated by the dashed-dotted lines in Fig. 5a. Thus, frequent hopping events between individual domains destroys the characteristic of the noise-free HDP scaling and causes the dif-

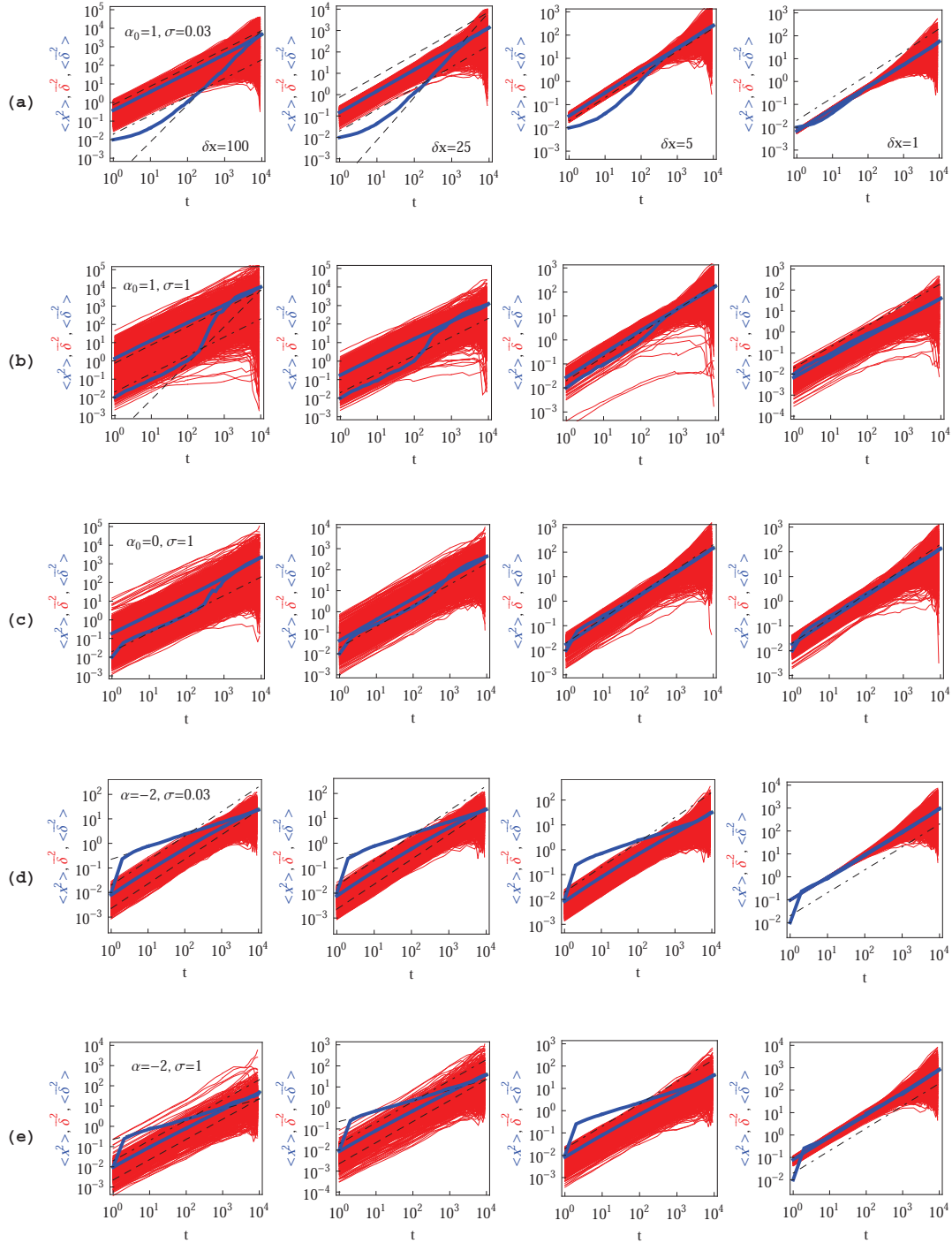


Figure 4: Ensemble and time averaged MSDs and amplitude scatter of individual traces  $\overline{\delta^2}$  for noisy HDPs with quenched disorder. The values of  $\alpha$ ,  $\sigma$ , and domain size  $\delta x$  are indicated in the plots. The panels (a) and (b) are for subdiffusive noisy HDPs, panel (c) stands for noisy Brownian motion, and panels (d) and (e) represent superdiffusive noisy HDPs. The MSD is computed with respect to the position of the center of the first domain,  $\langle (x(t) - x_{c,1})^2 \rangle$ . Parameters:  $T = 10^4$ ,  $N = 10^3$ , and  $\delta x$  values are the same in each column. The notations for the curves and asymptotes are the same as in Fig. 2.



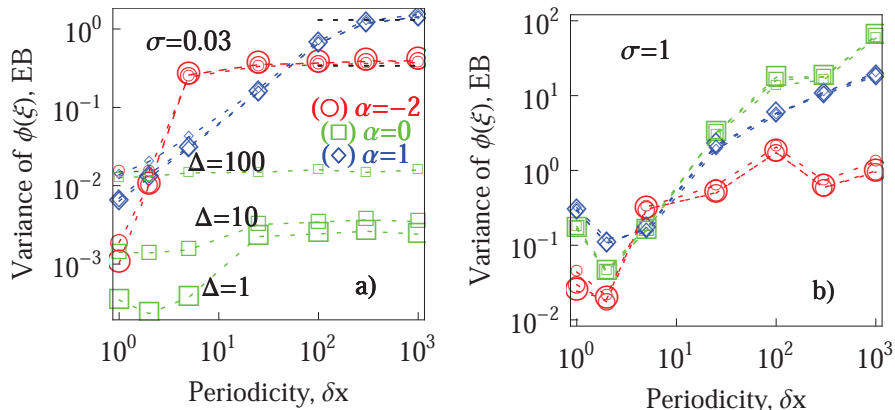


Figure 5: Ergodicity breaking parameter of noisy HDPs with quenched disorder. The parameters are the same as in Fig. 4, the values for  $\alpha$  and  $\sigma$  being indicated in the plots. The black dotted lines represent the ergodicity breaking parameter for the standard HDPs. The large, medium, and small symbols correspond to the lag times  $\Delta = 1, 10,$  and  $100$ , respectively.

fusion to be more ergodic. This is our second important conclusion.

For larger  $\sigma$  values the MSD stops following the HDP scaling law (1) and instead two nearly Brownian regimes are detected for short and long diffusion times, see the left panel in Fig. 4b. Similar to noisy CTRWs [7, 22], for noisy HDPs we observe a superposition of anomalous scaling for the MSD inherent to HDPs with the linear MSD increase due to particle jumping between the stratified domains. The latter term contributes stronger for smaller  $\delta x$  values: after a given number of steps  $T$  performed the particle visits more  $D(x)$  domains and its diffusion on the length scale  $\gg \delta x$  becomes effectively more normal and ergodic.

The time averaged MSD is an approximately linear function of the lag time  $\Delta$ . For smaller domain size  $\delta x$  we observe a more confined amplitude spread of the time averaged MSD traces  $\bar{\delta}^2$ , see the evolution from left to right in Figs. 4a,b. A similar behavior occurs for subdiffusive noisy HDPs, as demonstrated in Figs. 4d,e consistent with smaller values of the ergodicity breaking parameter. This is our third main result. For superdiffusive noisy HDPs, given large domain sizes  $\delta x$ , we observe more distant particle excursions and thus a broader amplitude spread of individual time traces  $\bar{\delta}^2(\Delta)$ , particularly for large values  $\sigma^2$  of the noise strength (Figs. 4e): at larger  $\sigma^2$  we correspondingly obtain larger values of the ergodicity breaking parameter, compare panels (a) and (b) in Fig. 5.

We find that the distribution  $\phi(\xi)$  of the amplitude scatter features a skewed form, which is characterized by its second, third, and fourth moments corresponding to the ergodicity breaking parameter, the skewness  $S$ , and the kurtosis  $K$ , respectively. For larger values of  $\sigma^2$ ,  $S(\xi)$  and  $K(\xi)$  grow with the domain size  $\delta x$  and are more irregular than the distribution  $\phi(\xi)$  itself, due to worsening statistics for higher order moments (not shown). Note that for short lag times  $\Delta/T \ll 1$  the ergodicity breaking parameter for large domain sizes  $\delta x$  approaches the values of the corresponding normal HDPs [33], compare Fig. 5a. At small domain size  $\delta x$  the non-ergodic properties of the standard HDPs are masked by the noise in the stratified spatial domains.

For superdiffusive HDPs the particles tend to localize in the center of each domain, while for subdiffusive values  $\alpha_0 < 0$  they tend to spread towards regions of low diffusivity near the domain borders. In the long time limit the particles spread over many domains, establishing the shape of the probability density function  $P(x, t)$  presented in Fig. 6. The local minima and maxima of  $P(x, t)$  correspond to the regions of low and fast diffusivity  $D(x)$ , respectively, see Figs. 1c,d and 6. For relatively large domain size  $\delta x$  the probability density function of the noisy HDPs becomes dominated by the contribution from the seed domain. The spreading of particles over superdiffusive HDP domains in the long time limit is symmetric

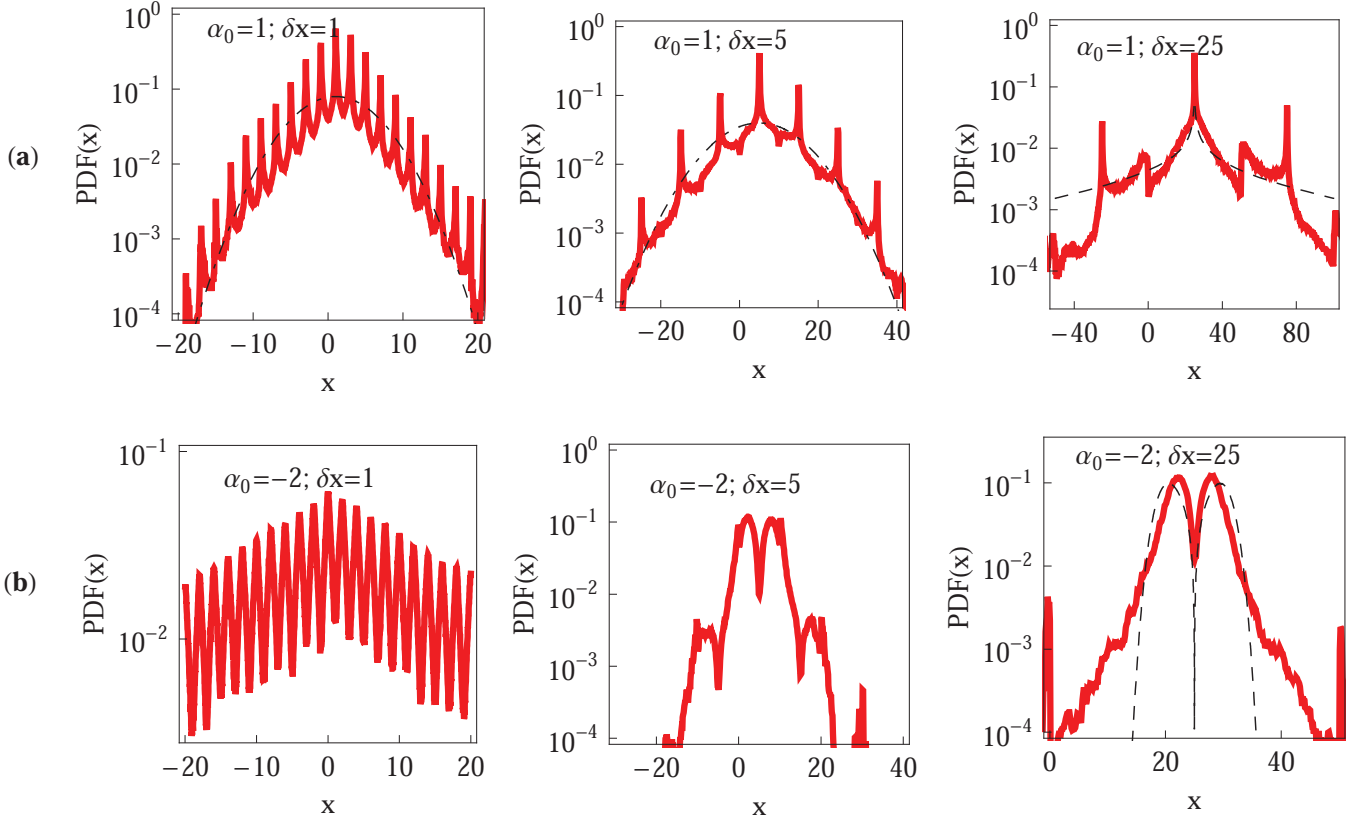


Figure 6: Probability density functions of noisy HDPs with quenched disorder for noise strength  $\sigma^2=1$  and varying domain size  $\delta x$ . The other parameters are the same as in Fig. 4. Panel (a) represents superdiffusive noisy HDPs and panel (b) stands for subdiffusive noisy HDPs. The shift of the peak positions with respect to those of the standard HDPs [33] is due to the shift ( $\delta x$ ) of the domain center positions, see Eq. (16). The dashed curves represent the probability density functions of standard HDPs, given by Eq. (12), while the dashed-dotted curves are result (20).

and nearly Gaussian,

$$P(x, t) = \frac{1}{\sqrt{4\pi D_{\text{eff}} t}} \exp\left(-\frac{(x - x_{c,1})^2}{4D_{\text{eff}} t}\right) \quad (20)$$

with the effective diffusivity  $D_{\text{eff}}$ . The mean particle displacement with respect to the center of the seed domain vanishes,  $\langle x(t \rightarrow \infty) \rangle \rightarrow 0$ . To compute  $D_{\text{eff}}$  analytically a homogenization procedure and generic concepts of diffusion in random and highly heterogeneous media would need to be applied [50].

### C. Subdiffusive noisy HDPs, $\alpha_0 = -2$

Subdiffusive noisy HDPs in the quenched scenario share a number of trends with the above descriptions of

the cases  $\alpha = 0$  and  $\alpha = 1$ . In particular, as the domain size  $\delta x$  decreases, the amplitude spread of individual time averaged MSD traces  $\overline{\delta^2}$  decreases (Fig. 4d,e). Because of the sublinear scaling of the ensemble MSD of the normal subdiffusive HDPs ( $\alpha_0 < 0$ ) the ensemble averaged MSD approaches the time averaged MSD  $\langle \overline{\delta^2(\Delta)} \rangle$  from above. Moreover, the scaling of the ensemble averaged MSD of subdiffusive noisy HDPs with quenched disorder turns from subdiffusive to Brownian as the domain size  $\delta x$  decreases. The physical reason for this crossover behavior is the random character of hops between domains with a varying local exponent  $\alpha$ . We find that, similarly to superdiffusive noisy HDPs, the ensemble averaged MSD initially follows the scaling (1) of normal HDPs while at later times a nearly linear scaling is observed. For smaller periodicities  $\delta x$  the linear scaling becomes dominant,

as demonstrated in Fig. 4e from left to right.

The probability density function of quenched noisy HDPs in the long time limit is a combination of the superimposed local probability densities of the standard HDP. For large periodicities  $\delta x$  the probability density function is again dominated by the contribution from the seed domain, as can be seen in the right panel of Fig. 6b. Similar to superdiffusive noisy HDPs we find that the time averaged MSD is linear in the lag time,  $\langle \delta^2(\Delta) \rangle \sim \Delta$ , while the amplitude spread of individual time averaged MSDs grows with the noise strength  $\sigma^2$  and becomes diminished for smaller medium periodicities  $\delta x$ . We also see that for subdiffusive noisy HDPs the saturation of the ergodicity breaking parameter to the values of normal HDPs occurs at much smaller values of  $\delta x$  as compared to superdiffusive noisy HDPs (Fig. 5a).

## VI. CONCLUSIONS

We studied a stochastic process based on a combination of heterogeneous diffusion processes with multiplicative noise and additional disorder of the environment, distinguishing annealed and quenched scenarios. The environment was assumed to be structured into periodic domains of given periodicity. We investigated the diffusive and ergodic properties of these noisy heterogeneous diffusion processes. The superposition of the additional stochasticity onto the standard HDP with its deterministic variation of the diffusivity revealed a variety of new features, the scaling relations for the ensemble and time averaged MSD of the noisy HDPs being dramatically altered as compared to the normal HDP behavior.

For annealed disorder, the scaling exponent  $\alpha$  of the diffusivity profile switches in time and the gradient field of the particle diffusivity has a single origin at  $x = 0$ . We demonstrated how the Gaussian spread  $p(\alpha)$  of the scaling exponent gives rise to a strongly asymmetric scatter of individual time averaged MSD traces. Rapidly switching diffusivity profiles in such an annealed environment cause transient particle trapping in low-diffusivity regions. For superdiffusive motion the effects of the  $\alpha$  spread are more pronounced. In the case of a quenched environment, a spatially stratified medium is modeled in terms of domains of width  $2\delta x$  with a normal distribution of the local HDP exponent. Upon particle diffusion, the averaging is thus performed over ensembles of particle trajectories generated for different spatial distributions of the scaling exponents  $\alpha$  in the domains. One of the key findings is that for small periodicity  $\delta x$  the sub- and superdiffusive scaling of normal HDPs cross over to a linear growth of the ensemble averaged MSD as function of time. External noise thus progressively masks the statistics of the underlying HDP.

What could be the physical phenomena captured by

the noisy HDP discussed here? From a biological perspective, the diffusion of small molecules in assemblies of non-identical, interconnected cells is a relevant example. The cell-to-cell variations of the diffusivity are inherent to biological tissues, while every individual cell features a space dependent diffusivity in its cytoplasm [8]. At cell-to-cell boundaries the diffusivity likely varies with a jump, as captured by our stratified model of the quenched disorder, with possibly discontinuous diffusivity across the system. We note that heterogeneous diffusivities can, for instance, play a role in the formation of gradients of morphogen molecules in a developing cell tissue [51], a process known to involve features of anomalous diffusion. It also features a division of fluxes of the molecules into fluxes through cells, across the outer cell membranes, and transport in extracellular spaces [52]. Heterogeneous diffusion of water molecules in brain tissues [53] and strongly heterogeneous structures of cardiac muscle tissue with nontrivial cell-cell coupling [54] could be another example. Similarly, the domains in the noisy HDP could represent internal compartments in a single cell. The quenched case would correspond to static environments whereas the annealed scenario would stand for environments, which change rapidly compared to the typical crossing times between domains.

Our results for noisy HDPs could also be useful for the description of nano-objects trapped in dynamical temperature fields [55] and of particles in strong temperature gradients [56]. Another field of relevance is the tracer diffusion in heterogeneous assemblies of distributed obstacles [57] mimicking features of the cell cytoplasm [8] and diffusion on chemically and mesoscopically periodically patterned solid-liquid interfaces [58]. On a macroscopic scale, water diffusion in subsurface hydrology applications is to be mentioned [12], as well as tracer motion in porous heterogeneous media [59]. For the latter there likely exists a distance-dependent diffusivity within each pore constructing a network governing the diffusion of water and contaminants in soil specimen [12]. Finally, in statistical models of financial stock price variations [60] the terms stochastic versus correlated volatility widely occur, representing the diffusivity in random walk models [61]. Some patterns of correlated or clustered volatility observed in financial data thus correspond to a systematically varying diffusivity in our model of quenched noisy HDPs. Some repeats of non-Brownian up-and-down trends in stock price fluctuations [61] can thus be considered as HDPs repeatedly occurring in time.

## Acknowledgments

We acknowledge funding from the Academy of Finland (FiDiPro scheme to RM) and the Deutsche Forschungsgemeinschaft (Grant CH 707/5-1 to AGC).

- [1] M. Weiss, H. Hashimoto, and T. Nilsson, *Biophys. J.* **84**, 4043 (2003); I. Golding and E. C. Cox, *Phys. Rev. Lett.* **96**, 098102 (2006); I. Bronstein, Y. Israel, E. Kepten, S. Mai, Y. Shav-Tal, E. Barkai, and Y. Garini, *Phys. Rev. Lett.* **103**, 018102 (2009); E. Kepten, I. Bronshtein, and Y. Garini, *Phys. Rev. E* **87**, 052713 (2013); A. V. Weigel, B. Simon, M. M. Tamkun, and D. Krapf, *Proc. Natl. Acad. Sci. U. S. A.* **108**, 6438 (2011); S. M. A. Tabei, S. Burov, H. Y. Kim, A. Kuznetsov, T. Huynh, J. Jureller, L. H. Philipson, A. R. Dinner, and N. F. Scherer, *Proc. Natl. Acad. Sci. U. S. A.* **110**, 4911 (2013); J.-H. Jeon, V. Tejedor, S. Burov, E. Barkai, C. Selhuber-Unkel, K. Berg-Sorensen, L. Oddershede, and R. Metzler, *Phys. Rev. Lett.* **106**, 048103 (2011); M. A. Taylor, J. Janousek, V. Daria, J. Knittel, B. Hage, H.-A. Bachor, and W. P. Bowen, *Nature Phot.* **7**, 229 (2013).
- [2] D. S. Banks and C. Fradin, *Biophys. J.* **89**, 2960 (2005); J. Szymanski and M. Weiss, *Phys. Rev. Lett.* **103**, 038102 (2009); G. Guigas, C. Kalla and M. Weiss, *Biophys. J.* **93**, 316 (2007); J.-H. Jeon, N. Leijnse, L. B. Oddershede, and R. Metzler, *New J. Phys.* **15**, 045011 (2013); W. Pan, L. Filobelo, N. D. Q. Pham, O. Galkin, V. V. Uzunova, and P. G. Vekilov, *Phys. Rev. Lett.* **102**, 058101 (2009).
- [3] J. Mattsson, H. M. Wyss, A. Fernandez-Nieves, K. Miyazaki, Z. B. Hu, D. R. Reichman, and D. A. Weitz, *Nature* **462**, 83 (2009); E. R. Weeks, J. C. Crocker, A. C. Levitt, A. Schofield, and D. A. Weitz, *Science* **287**, 627 (2000).
- [4] E. Yamamoto, T. Akimoto, M. Yasui and K. Yasuoka, *Sci. Rep.* **4**, 4720 (2014); G. R. Kneller, K. Baczynski, and M. Pasienkewicz-Gierula, *J. Chem. Phys.* **135**, 141105 (2011); J.-H. Jeon, H. Martinez-Seara Monne, M. Javanainen, and R. Metzler, *Phys. Rev. Lett.* **109**, 188103 (2012); M. Javanainen, H. Hammaren, L. Monticelli, J.-H. Jeon, R. Metzler, and I. Vattulainen, *Faraday Discussions* **161**, 397 (2013).
- [5] R. Metzler and J. Klafter, *Phys. Rep.* **339**, 1 (2000).
- [6] F. Höfling and T. Franosch, *Rep. Progr. Phys.* **76**, 046602 (2013).
- [7] R. Metzler, J.-H. Jeon, A. G. Cherstvy, and E. Barkai, *Phys. Chem. Chem. Phys.* **16**, 24128 (2014).
- [8] T. Kühn, T. O. Ihalainen, J. Hyväluoma, N. Dross, S. F. Willman, J. Langowski, M. Vihinen-Ranta, and J. Timonen, *PLoS ONE* **6**, e22962 (2011).
- [9] B. P. English, V. Hauryliuk, A. Sanamrad, S. Tankov, N. H. Dekker, and J. Elf, *Proc. Natl. Acad. Sci. U. S. A.* **108**, E365 (2011).
- [10] I. Y. Wong, M. L. Gardel, D. R. Reichman, E. R. Weeks, M. T. Valentine, A. R. Bausch, and D. A. Weitz, *ibid.* **92**, 178101 (2004).
- [11] A. Godec, M. Bauer, and R. Metzler, *New J. Phys.* **16**, 092002 (2014); compare the experiments in C. H. Lee, A. J. Crosby, T. Emrick, and R. C. Hayward, *Macromol.* **47**, 741 (2014).
- [12] H. Scher, G. Margolin, R. Metzler, J. Klafter, and B. Berkowitz, *Geophys. Res. Lett.* **29**, 1061 (2002); M. Dentz et. al., *Adv. Water Res.* **49**, 13 (2012); R. Haggerty and S. M. Gorelick, *Water Resour. Res.* **31**, 2383 (1995); B. Berkowitz, A. Cortis, M. Dentz, and H. Scher, *Rev. Geophys.* **44**, RG2003 (2006); B. Berkowitz and H. Scher, *Transp. Porous Media*, **42**, 241 (2001).
- [13] J.-P. Bouchaud and A. Georges, *Phys. Rep.* **195**, 127 (1990).
- [14] S. Havlin and D. Ben-Avraham, *Adv. Phys.* **51**, 187 (2002).
- [15] J. W. Haus and K. W. Kehr, *Phys. Rep.* **150**, 263 (1987).
- [16] J. P. Bouchaud, A. Comtet, A. Georges, and P. le Doussal, *Ann. Phys.* **201**, 285 (1990).
- [17] G. C. Papanicolaou, *Diffusion in random media, Surveys in applied mathematics*, pp. 205-253 (Plenum Press, New York, NY 1995).
- [18] T. H. Solomon, E. R. Weeks and H. L. Swinney, *Phys. Rev. Lett.* **71**, 3975 (1993); G. M. Zaslavsky, *Phys. Rep.* **371**, 461 (2002); G. M. Zaslavsky, *Hamiltonian Chaos and Fractional Dynamics* (Oxford University Press, Oxford UK, 2005); G. Zumofen and J. Klafter, *Phys. Rev. E* **47**, 851 (1993).
- [19] S. Burov and E. Barkai, *Phys. Rev. Lett.* **98**, 250601 (2007); C. Monthus and J.-P. Bouchaud, *J. Phys. A: Math. Gen.* **29**, 3847 (1996); E. Bertin and J.-P. Bouchaud, *Phys. Rev. E* **67**, 026128 (2003).
- [20] T. Akimoto and E. Barkai, *Phys. Rev. E* **87**, 032915 (2013); T. Akimoto and T. Miyaguchi, *Phys. Rev. E* **82**, 030102 (2010); T. Akimoto, *Phys. Rev. Lett.* **108**, 164101 (2012); T. Geisel and S. Thomae, *Phys. Rev. Lett.* **52**, 1936 (1984); T. Geisel, J. Nierwetberg and A. Zacherl, *Phys. Rev. Lett.* **54**, 616 (1985);
- [21] A. M. Berezhkovskii, L. Dagdug, and S. M. Bezrukov, *Biophys. J.* **106**, L09 (2014).
- [22] J.-H. Jeon, E. Barkai, and R. Metzler, *J. Chem. Phys.* **139**, 121916 (2013).
- [23] P. Massignan, C. Manzo, J. A. Torreno-Pina, M. F. García-Parako, M. Lewenstein, and G. L. Lapeyre, Jr., *Phys. Rev. Lett.* **112**, 150603 (2014).
- [24] M. V. Chubynsky and G. W. Slater, *Phys. Rev. Lett.* **113**, 098302 (2014).
- [25] J.-P. Bouchaud, *J. Phys. I* **2**, 1705 (1992); G. Bel and E. Barkai, *Phys. Rev. Lett.* **94**, 240602 (2005); A. Rebenishtok and E. Barkai, *ibid.* **99**, 210601 (2007); A. Lubelski, I. M. Sokolov and J. Klafter, *Phys. Rev. Lett.* **100**, 250602 (2008); I. M. Sokolov, E. Heinsalu, P. Hänggi, and I. Goychuk, *Europhys. Lett.* **86**, 041119 (2010); M. A. Lomholt, I. M. Zaid, and R. Metzler, *Phys. Rev. Lett.* **98**, 200603 (2007); G. Aquino, P. Grigolini, and B. J. West, *Europhys. Lett.* **80**, 10002 (2007) M. Khoury, A. M. Lacasta, J. M. Sancho, and K. Lindenberg, *Phys. Rev. Lett.* **106**, 090602 (2011).
- [26] Y. He, S. Burov, R. Metzler, and E. Barkai, *Phys. Rev. Lett.* **101**, 058101 (2008).
- [27] E. Barkai, Y. Garini, and R. Metzler, *Physics Today* **65**(8), 29 (2012).
- [28] S. Burov, J.-H. Jeon, R. Metzler and E. Barkai, *Phys. Chem. Chem. Phys.* **13**, 1800 (2011).
- [29] I. M. Sokolov, *Soft Matter* **8**, 9043 (2012).
- [30] A. Y. Khinchin, *Mathematical foundations of statistical mechanics* (Dover Publications Inc., New York, NY, 2003).
- [31] S. Burov, R. Metzler, and E. Barkai, *Proc. Natl. Acad. Sci. USA* **107**, 13228 (2010).
- [32] A. Fulinski, *J. Chem. Phys.* **138**, 021101 (2013); *Phys. Rev. E* **83**, 061140 (2011).
- [33] A. G. Cherstvy, A. V. Chechkin, and R. Metzler, *New J.*

- Phys. **15**, 083039 (2013).
- [34] A. G. Cherstvy, A. V. Chechkin, and R. Metzler, *Soft Matter* **10**, 1591 (2014).
- [35] A. G. Cherstvy and R. Metzler, *Phys. Rev. E* **90**, 012134 (2014); A. G. Cherstvy, A. V. Chechkin, and R. Metzler, *J. Phys. A* **47**, 485002 (2014).
- [36] A. G. Cherstvy and R. Metzler, *Phys. Chem. Chem. Phys.* **15**, 20220 (2013).
- [37] E. Barkai, *Phys. Rev. Lett.* **90**, 104101 (2003); E. Barkai and Y. C. Cheng, *J. Chem. Phys.* **118**, 6167 (2003); J. H. P. Schulz, E. Barkai, and R. Metzler, *Phys. Rev. Lett.* **110**, 020602 (2013); *Phys. Rev. X* **4**, 011028 (2014).
- [38] H. Safdari, A. V. Chechkin, G. R. Jafari, and R. Metzler, E-print arXiv:1501.04810.
- [39] N. G. van Kampen, *Stochastic processes in physics and chemistry* (Elsevier, Amsterdam, 2007).
- [40] Y. Meroz, I. M. Sokolov, and J. Klafter, *Phys. Rev. E* **81**, 010101(R) (2010).
- [41] W. Deng and E. Barkai, *Phys. Rev. E* **79**, 011112 (2009). J.-H. Jeon and R. Metzler, *Phys. Rev. E* **81**, 021103 (2010).
- [42] G. Kneller, *J. Chem Phys.* **141**, 041105 (2014); I. Goychuk, *Phys. Rev. E* **80**, 046125 (2009); *Adv. Chem. Phys.* **150**, 187 (2012).
- [43] Note, however, that transient deviations from the ergodic behavior exist in confinement: J.-H. Jeon and R. Metzler, *Phys. Rev. E* **85**, 021147 (2012); J.-H. Jeon, N. Leijnse, L. B. Oddershede, and R. Metzler, *New J. Phys.* **15**, 045011 (2013); J. Kursawe, J. Schulz, and R. Metzler, *Phys. Rev. E* **88**, 062124 (2013).
- [44] V. Tejedor and R. Metzler, *J. Phys. A* **43**, 082002 (2010); M. Magdziarz, R. Metzler, W. Szczotka, and P. Zebrowski, *Phys. Rev. E* **85**, 051103 (2012).
- [45] J.-H. Jeon, A. V. Chechkin and R. Metzler, *Phys. Chem. Chem. Phys.* **16**, 15811 (2014).
- [46] F. Thiel and I. M. Sokolov, *Phys. Rev. E* **89**, 012115 (2014).
- [47] A. G. Cherstvy and R. Metzler, E-print arXiv:1502.01554.
- [48] A. Godec, A. V. Chechkin, E. Barkai, H. Kantz, and R. Metzler, *J. Phys. A* **47**, 492002 (2014); L. P. Sanders, M. A. Lomholt, L. Lizana, K. Fogelmark, R. Metzler, and T. Ambjörnsson, *New J. Phys.* **16**, 113050 (2014); M. A. Lomholt, L. Lizana, R. Metzler, and T. Ambjörnsson, *Phys. Rev. Lett.* **110**, 208301 (2013).
- [49] D. Froemberg and E. Barkai, *Phys. Rev. E* **87**, 030104(R) (2013); *Phys. Rev. E* **88**, 024101 (2013); *Euro. Phys. J. B* **86**, 331 (2013); A. Godec and R. Metzler, *Phys. Rev. Lett.* **110**, 020603 (2013); *Phys. Rev. E* **88**, 012116 (2013); G. Zumofen and J. Klafter, *Physica D* **69**, 436 (1993).
- [50] R. E. Showalter and D. B. Visarraga, *J. Math. Anal. Appl.* **295**, 191 (2004).
- [51] K. Kruse and A. Iomin, *New J. Phys.* **10**, 023019 (2008).
- [52] H. Berry and H. A. Soula, *Front. Physiol.* **5**, 437 (2014); H. Berry and H. Chate, *Phys. Rev. E* **89**, 022708 (2014).
- [53] C. Nicholson, *Rep. Prog. Phys.* **64**, 815 (2001); E. Sykova and C. Nicholson, *Physiol. Reviews* **88**, 1277 (2008); D. S. Novikov, J. H. Jensen, J. A. Helpert, and E. Fieremans, *Proc. Natl. Acad. Sci. U.S.A.* **111**, 5088 (2014).
- [54] A. Bueno-Orovio et al., *J. R. Soc. Interface* **11**, 20140352 (2014).
- [55] M. Braun, A. Wuerger and F. Cichos, *Phys. Chem. Chem. Phys.* **16**, 15207 (2014).
- [56] C. B. Mast, S. Schink, U. Gerland, and D. Braun, *Proc. Natl. Acad. Sci. U.S.A.* **110**, 8030 (2013).
- [57] S. K. Ghosh, A. G. Cherstvy, and R. Metzler, *Phys. Chem. Chem. Phys.* **17**, 472 (2015); S. K. Ghosh, A. G. Cherstvy, and R. Metzler, work in preparation.
- [58] M. J. Skaug, A. M. Lacasta, L. Ramirez-Piscina, J. M. Sancho, K. Lindenberg, and D. K. Schwartz, *Soft Matter* **10**, 753 (2014).
- [59] D. L. Koch and J. F. Brady, *Phys. Fluids* **31**, 965 (1988).
- [60] J.-P. Bouchaud and M. Potters, "Theory of Financial Risks", Cambridge University Press, (2000); R. N. Mantegna and H. E. Stanley, "Introduction to Econophysics: Correlations and Complexity in Finance", Cambridge University Press, (2000).
- [61] K. Yamasaki, L. Muchnik, S. Havlin, A. Bunde, and H. E. Stanley, *Proc. Natl. Acad. Sci. U.S.A.* **102**, 9424 (2005).